Laser cladding and wear testing of nickel base hardfacing materials: Influence of process parameters

P. Aubry[a] and C. Blanc
Den–Service d'Etudes Analytiques et de Réactivité des Surfaces (SEARS), CEA, Université Paris-Saclay, F-91191 Gif-sur-Yvette, France

I. Demirci
MSMP, Ecole Nationale Supérieure d'Arts et Métiers, Châlons-en-Champagne 5006, France

M. Dal and T. Malot
PIMM, Ecole Nationale Supérieure d'Arts et Métiers, Paris 75013, France

H. Maskrot
Den–Service d'Etudes Analytiques et de Réactivité des Surfaces (SEARS), CEA, Université Paris-Saclay, F-91191 Gif-sur-Yvette, France

In fast neutron reactors, some parts can be subjected to displacements between each other (as movable parts for example). On these parts, the contact areas usually need a hardfacing coating. The standard hardfacing alloy is a cobalt-base alloy (for example Stellite®6). Unfortunately, in the primary coolant circuit and on wear conditions, cobalt can be released. Under neutron flux, the stable ^{59}Co can be transmuted into ^{60}Co by radioactive capture of neutrons and, therefore, can contaminate the primary circuit. Therefore, it is desired to replace this cobalt based hardfacing alloy by a cobalt-free one. Previous presentations have shown the potential interest of some nickel base materials as Colmonoy® alloy. In parallel, laser cladding has been identified as a deposition process that could increase the performances of the hardfacing materials compared to the standard process (Plasma Transferred Arc Welding). In all the study, the base material is the stainless steel 316LN. In the first section of this article, the authors present previous results related to the selection of hardfacing materials and their evaluation in comparable tribology conditions. Then, Tribaloy® 700, another nickel based alloy that has been poorly investigated, is presented and evaluated. This nickel base has a completely different microstructure, and its tribological behavior related to the variation of the microstructure is not well known. First, the authors present the features of the selected materials. Then, the authors present various property characterization results obtained by changing several process parameters. The quality of the clad is considered, and the process window providing a good clad is determined (no crack, only a few porosities, etc.). The variation of the microstructure is analyzed, and solidification paths are proposed regarding the process parameters. Wear tests are performed on typical wear conditions. The movement is linear. Argon is used for the protection of the sample against oxidation. Tests are carried out at 200 °C. Wear tests are analyzed, and wear mechanisms are correlated with the microstructure of the material.

Key words: nuclear applications, laser cladding, hardfacing materials, stellite, nickel base alloys, wear resistance, galling

I. INTRODUCTION

The CEA is responsible on behalf of France for leading research on innovative nuclear systems, called Generation IV, which integrate major technological breakthroughs compared to the previous generation of reactors. From 2010, the CEA is leading the ASTRID project, an Advanced Sodium Fast Reactor for Industrial Demonstration, currently in its conceptual design phase. One part of the project (the subproject MASNA) is related to the studies on structure materials and particularly to the selection of the hardfacing materials that will be used in contact and mobile zones.

The main feature of Fast Neutron Reactors in the field of tribology is due to the use of liquid sodium, which has the ability to reduce many metal oxides. This avidity depends on the nature of the oxides and the temperature. For reasons related on the one hand to the risk of clogging of pipes and on the other hand to corrosion and transfer of activation products, it is necessary to purify the primary and secondary sodium by passing it through cold traps. The more the purification of liquid sodium is pushed toward the low concentrations of oxygen, the less the formation of self-lubricant mixed oxides such as chromite or sodium aluminate is probable. Therefore, the minimum concentration of oxygen in the sodium is fundamental for tribology.

The first hardfacing materials used to overcome the problems of friction in sodium are cobalt based alloys,

[a]Electronic mail: pascal.aubry@cea.fr

commonly used in several industrial fields. However, one major drawback of these alloys for nuclear applications is the activation of Cobalt under neutron flux in a reaction ^{59}Co (n, γ) $\rightarrow$ ^{60}Co. With a period of 5.7 years, the activity of Cobalt 60 is maximum during operation of the reactor. A period of at least 30 years after the shutdown is necessary to observe a significant reduction in induced activity. Thus, it is desirable to avoid these alloys for severe neutron flow and different studies that tried to find a substitute material without cobalt or in very small quantities.

There are different areas in sodium fast reactor that have been identified as being most affected by friction (wear): the strongback support on the primary vessel, candle assembly components, steam generator components, moving parts in valves, etc.

The requirements are very demanding: tribo-corrosion under sodium, operating temperature from 180 to 500 °C, risk of thermal shock and thermal cycling, and life span of over 60 years without binding or degradation.

II. SELECTION OF MATERIALS

The context of the future reactor implies a number of constraints on the possible choice of hardfacing materials. Particularly, the range of temperatures between 200 and 500 °C during operation is very constraining for the selection of hardfacing alloys. First, it has been decided to keep, as a reference, Stellite 6 alloy, a cobalt-based material.

A. Substrate material

After initial analysis of the possible zones that could be subject to wear in the Sodium Fast Reactor, it has been decided to focus the study on reactor vessel and core structural components. The base material has to be selected for its main characteristics against the operating conditions: good creep at high temperature, sodium compatibility (i.e., Na corrosion resistance), good irradiation behavior (low deformation under neutron flow), cost, etc. Different stainless steel alloys have been used in the existing reactor. Particularly, the AISI 316 alloys are encountered in different reactors for their good properties. In our project, 316L and 316LN have been selected as base materials for laser cladding of the hardfacing alloys.

Considering the contact zones that can be found in the reactor, it is clear that a 316L(N)/316L(N) contact is not a good couple for sliding conditions. Therefore, it is required to coat almost one side of the contact (commonly, the static part) in order to get a hardfacing material/316L(N) contact. This will be the system considered in the tribological study.

B. Stellite® alloys

Stellite is the well known and widely used hardfacing wear resistance material. The Stellite alloy, from Deloro Company, is a cobalt-chromium base especially designed for abrasion resistance. There are many alloys of Stellite composed of variable proportions of cobalt, nickel, iron, aluminum, boron, carbon, chromium, manganese, molybdenum, phosphorus, sulfur, silicon, and titanium, with most alloys having four to six of these elements.

Stellite alloys have a high melting point and high hardness (e.g., Stellite 6:40 HRC; melting point 1260–1357 °C). They are therefore very difficult to machine. The hardness is strongly dependent on the microstructure. The ductility of Stellite is mainly determined by the volume fraction of carbides and their morphologies. An increase in the volume of carbides reduces ductility. Under conditions of oxidation, the elements Cr and Co can form chromium and cobalt oxides at different oxidation levels (see Refs. 1 and 2). The abrasion resistance is proportional to the hardness and increases with the proportion and the size of carbides (see Refs. 3 and 4).

A large number of Stellite substitutes have been proposed in the literature. Considering requirements, thick coatings are preferably retained. Among them, we can consider two main types of materials: the iron or nickel based alloys. If iron base alloys cannot be definitely excluded, the bibliography[5–7] mainly demonstrates the poor behavior of the iron-based hardfacing coatings at high temperature regardless of the deposition process.

In contrast, the authors have evidenced the interest of using Nickel based alloys for replacing the Cobalt based ones (see Refs. 8 and 9). Because of that, we have selected two promising nickel base alloys: Colmonoy® and Tribaloy®.

C. Colmonoy alloys

The Colmonoy is a nickel-based alloy developed by Wall colmonoy Company, which comprises hardening chromium borides and carbides. Its main interest is to be Cobalt free while providing different grades adapted to different wear and corrosion conditions. Laser cladding of Colmonoy 52 alloy has been investigated and presented in previous articles.[10–13]

If the Colmonoy 52 is still considered as a candidate as a Cobalt free hardfacing material, these previous results have demonstrated the difficulty in obtaining crack free deposits with high energy processes as Plasma Transferred Arc Welding (PTAW) or laser cladding, the two processes selected in the research project. Moreover, its wear behavior is clearly inferior to the Stellite 6 one.

D. Tribaloy alloys

Tribaloy alloys have been developed by the Deloro Company. Grades are offered in nickel or cobalt base. They are particularly useful in the case of dried metal-metal tribo-corrosion at high temperature (800–1000 °C). These grades have been developed to obtain a wear and corrosion behavior very close to Stellite. They may also contain a small proportion of cobalt.

Tribaloy T-700 (see Table I for composition) has a high resistance to corrosion and oxidation. It contains no cobalt and has been identified as a good candidate for nuclear applications. Note that its wear resistance is proportional to the volume fraction of the Laves phase present in the deposited material. Therefore, the results of wear tests are very sensitive to the process as the dilution rate, cooling rate, and overall thermal history of the clad.

TABLE I. Composition of different hardfacing alloys.

	Materials (wt. %)			
Chemical composition	AISI 316L	Stellite 6	Colmonoy 52	Tribaloy 700
B	—	—	2.2	—
C	0.02	0.9–1.4	0.55	<0.5
Co	—	Bal.	—	—
Cr	16–18	27–32	12.3	26
Fe	Bal.	—	3.8–4.8	<2.0
Mn	2–2.5	—	—	—
Mo	2	—	—	26
Ni	10.5–13.5	—	Bal.	Bal.
Si	1	—	3.7	<1.5
W	—	4–6	—	—

The microstructure of the Tribaloy 700 coating comprises the Laves-phase whose volume is about 60% (see Fig. 1). Thanks to this phase, this coating has good wear resistance.

The composition of the substrate (AISI 316L) and the three hardfacing materials (the Stellite is used as a reference) are presented in Table I.

III. SELECTION OF PROCESS PARAMETERS FOR LASER CLADDING OF TRIBALOY 700

Thick hardfacing coatings are obtained mainly by a fusion process if full density and metallurgical bounding are required as in our case. Among them, the PTAW is mostly used, qualified, and considered as the nominal process for this type of application.

However, compared to conventional fusion processes, laser cladding can provide very desirable properties: the dilution of the substrate can be accurately controlled and reduced and high solidification speed and thermal gradient can give a very fine microstructure with homogeneous properties and higher hardness (Ref. 14).

Therefore, we have decided to propose to deposit the selected materials by laser cladding as an alternative process that could improve the material properties. Comparison of the resulting properties of the deposits (microstructure and wear) between laser cladding and PTAW will be made when data from the PTAW process are available.

Previous results on laser cladding of Stellite 6 and Colmonoy 52 have been presented in Ref. 10. Therefore, this article presents the recent experiments and analysis achieved on Tribaloy 700.

A. Experimental setup

The laser cladding process has a large number of parameters that can influence the quality of the clad tracks. It involves a lot of parameters. Among them, three main parameters are the speed processing, the powder feeding rate, and the laser power.

The experimental setup is shown in Fig. 2. In this project, a continuous 10 kW Trumpf Disk laser was used to make deposits.

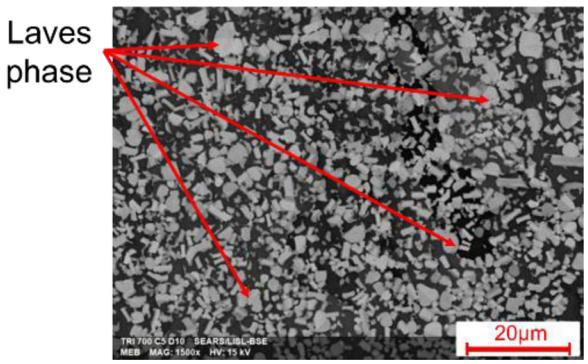

FIG. 1. Laves phase in the Tribaloy-700 coating deposited by laser cladding.

The laser beam is at the center of the cladding nozzle. The metal powder is transported by a gas stream and injected coaxially into the melt pool. One part of the powder flow can be heated by the laser before dropping in the melt pool. An argon inert gas protection surrounding the melt pool was used to avoid oxidation. The substrate is preheated by induction. The inductor has been designed to fully surround the sample and create a very homogeneous heating area in the substrate. The temperature used is between 200 and 550 °C. It is monitored by a pyrometer and a closed loop on the induction system. A precision of better than ±20 °C can be obtained.

B. Parameter search

1. General overview

For the experiments, specimens of 316L steel ($50 \times 50 \times 10$ and $200 \times 50 \times 20$ mm) have been used as substrates. The objective of the parameter search is to obtain sound deposits of Tribaloy 700 of a minimum of 4 mm. This means that the parameter search is made in order to find a set of parameters able to produce deposits with the following characteristics:

- Desired microstructure: initial parameter set is selected following an initially desired microstructure;
- Low number of porosities: if most of the time porosities cannot be completely avoided, it is likely desirable to produce deposits with a low number of porosities of small diameter;
- No lack of fusion: lack of fusion is likely to be avoided by a proper selection of the parameters controlling the shape of the track and the distance between tracks that could generate remaining gaps after solidification.

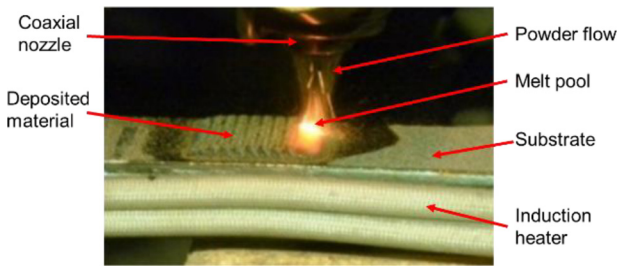

FIG. 2. Laser cladding setup. View during cladding.

- No cracks: hardfacing materials as nickel based alloys are rather brittle materials and can be subject to cold cracking during laser cladding. In that case, avoiding cracks is mainly achieved by controlling the thermal cycles during laser cladding, for example, by heating the substrate;
- Low dilution: process parameters must be selected in order to minimize the dilution zone at the interface between the substrate and the cladded material;
- Limited stress and distortion: the cladding process induces stress and deformation of the material. This must be limited in the acceptable range that depends on the application (materials, 3D shape, deposition area, etc.).

The main process parameters considered here are the laser power, the laser spot size, the travel speed, and the powder flow rate. Following the requirements, the parameter search is conducted as follows:

1. single track parameter search leading to the desired microstructure, good geometry, and low porosity (in addition the powder control);
2. multitrack strategy search: optimization of overlapping and adjustment of dilution;
3. reduction of cracks (if needed), by heating the substrate.

Of course, the process parameters are adjusted in each step of the parameter search in order to satisfy the requirements. In our parameter search, initial single tracks of about 1.5–5 mm thickness have been performed by tuning the laser spot size onto the substrate in order to generate an acceptable melt pool geometry (typical aspect ratio height/width ∼2/5–2/3).

After steps 1 and 2, a parameter window has been kept large enough in order to evaluate the influence of heating:

- Laser Power (P): 600–2000 W;
- Travel Speed (V): 400–1000 mm/min;
- Powder Flow (D): 5–40 g/min.

Now, we present the main causes of defects and the solutions to avoid them.

2. Porosity

The powder grain distribution is a standard one, 45–150 μm. The Tribaloy 700 powder used for the experiments presents a very low number of porosities in the grains (see Fig. 3).

This depends on the method of powder production. As we can see in Fig. 3, the powder exhibits mainly no occluded porosities and shows a very fine Laves phase structure due to rapid solidification.

As it is often seen, decreasing the size of the melt pool tends to increase the number of porosities of the clad. In our case, the number of porosities is very low thanks to the quality of the powder and a good tuning of the process parameters (adapted size and good stability of the hydrodynamics of the melt pool).

3. Crack and deformation

In the initial trials, the produced clads exhibit cracks. After analysis, it is clear that these cracks are not coming

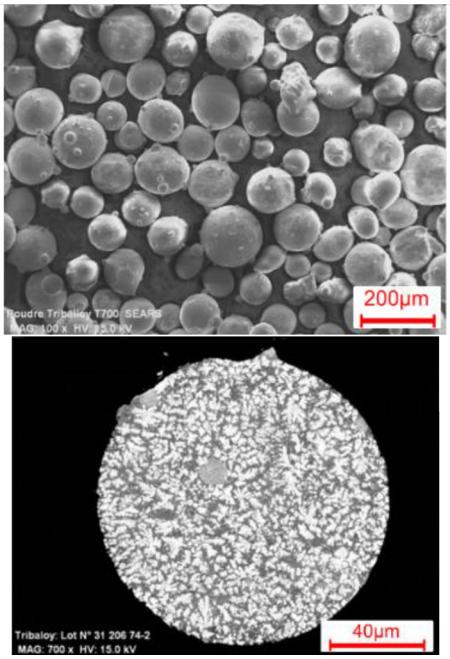

FIG. 3. Micrography of the Tribaloy 700 powder selected in the study (top: global view and bottom: view of a grain).

from hot cracking but certainly from stress produced during the clad. In order to avoid this, it has been considered to preheat the substrate between 500 and 600 °C (see Fig. 4) and cool the substrate with a low cooling rate after the cladding process. As it can be seen in Fig. 4, increasing the heating temperature dramatically enlarges the crack-free process parameter window.

Finally, among the sound deposits (no cracks, few porosities, and low dilution), two different Tribaloy 700 samples have been selected for wear evaluation. Finally, two samples

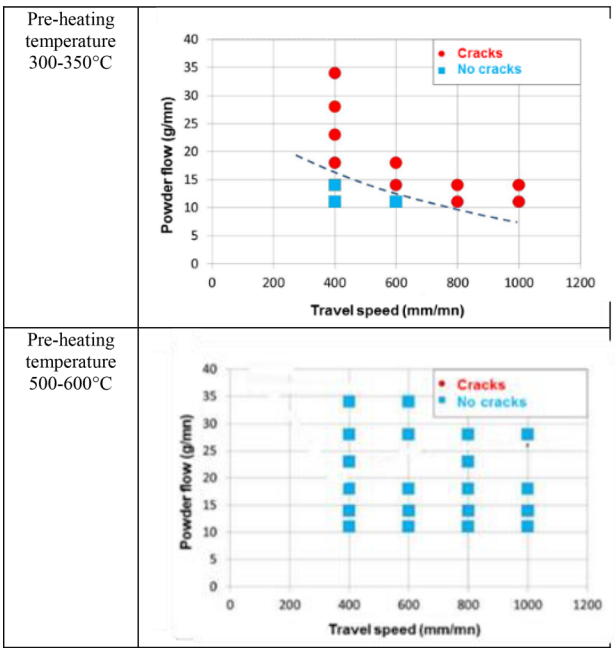

FIG. 4. Influence of the heating temperature on crack formation on Tribaloy 700 as a function of the powder flow rate (g/min) and travel speed (mm/min).

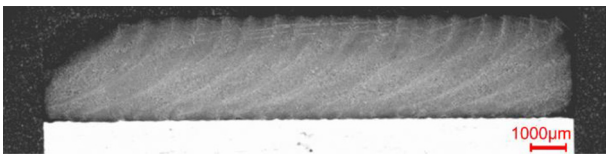

FIG. 5. Optical micrography of a vertical section of a typical laser clad of Tribaloy700.

with two extreme values of travel speed, achieved at a laser power of 2000W and heated at 500 °C, have been selected:

- $V = 400$ mm/min and $D = 14$ g/min: Tribaloy-C1,
- $V = 1000$ mm/min and $D = 21$ g/min: Tibaloy-C2.

These samples will used for the rest of the analysis.

4. Dilution

At a low travel speed (80–150 mm/min) and a low powder flow rate (2–5 g/min), the dilution is important and the transition between the substrate and the clad is quite smooth. The iron content increases from about 10% to the 316L iron content in about 1 mm. When increasing the travel speed to 200–500 mm/min to 1 m/min, the dilution is decreased. The iron content in the clad slightly decreases about 2% instead of 3.8% in the powder. Moreover, the dilution zone is reduced to less than 200 μm. In the samples made by laser cladding, the interface shows a good metallurgical bounding and continuity without defects (Fig. 5).

The transition zone is between 50 and 100 μm thickness (see Fig. 6 (top)). For the PTAW sample, the transition zone is about 900 μm thick (Fig. 6 (bottom)), showing a high dilution and leading to a high level iron content in the deposit.

C. Microstructural analysis

The microstructure and chemical composition of the cladding layers have been examined using a scanning electron microscope (SEM)/backscattered electrons (BSE) and SEM-SEM/electronic dispersive spectroscopy (EDS). They play a crucial role in determining the properties of a component. In this study, different zones (top surface, cross-section) were observed in detail to study the morphology of layers and the chemical composition.

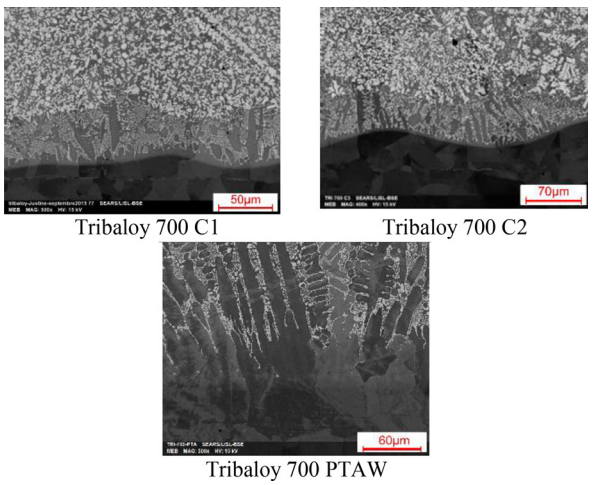

FIG. 6. SEM/BSE images at the interface of the laser clad of Tribaloy 700 deposited by the laser (C1 and C2) and PTAW.

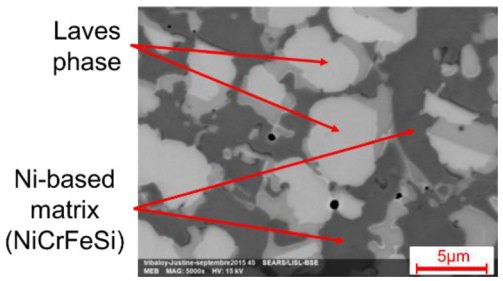

FIG. 7. SEM/BSE images of the Tribaloy-C1 sample.

The microstructure of the Tribaloy 700 coating consists of a Nickel-based matrix (NiCrMoSiFe) and two intermetallic phases (see Fig. 7, view of a top part of the clad). The energy-dispersive X-ray (EDX) results show that the difference between these intermetallic precipitates is very slight.

The cladding process presents a finer solidification microstructure (for example, size and distribution of the precipitates) than the solidification microstructure of the PTAW sample. Between both the microstructures from the laser process, the finest microstructure is subtracted at a high deposition speed (Tribaloy-C2).

Figure 8 presents the micrographies of Tribaloy 700 in the middle of the interface by laser cladding (Fig. 8 (top)) and PTAW (Fig. 8 (bottom)), respectively.

The microstructure of the laser cladded samples appears similar to the PTAW one, but slightly more homogeneous and finer. The Trivbaloy-C2 exhibits a finer microstructure than the Tribaly-C1 (about a factor of 2 for the first interdendritic distance). This is certainly due to the higher travel speed that induces a higher maximal solidification speed.

Figure 9 presents the micrographies (laser cladding and PTAW) of the microstructure of Tribaloy 700 in the upper part of the samples.

As it can been seen in Table II related to EDX analysis of each region of the image in Fig. 7, Laves precipitate is still

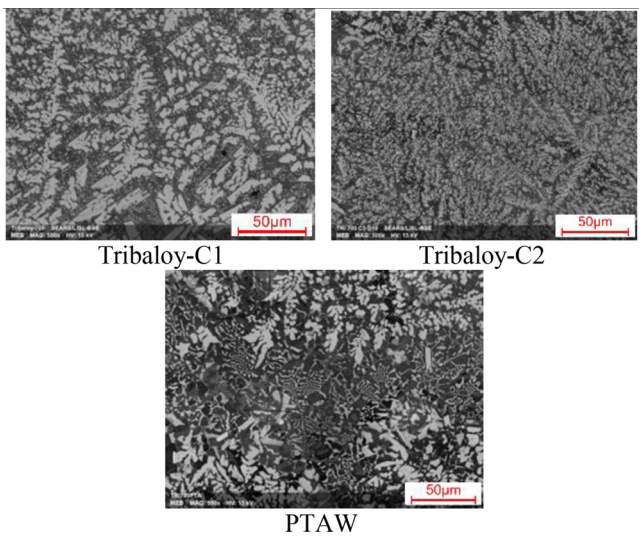

FIG. 8. SEM/BSE images of Tribaloy.

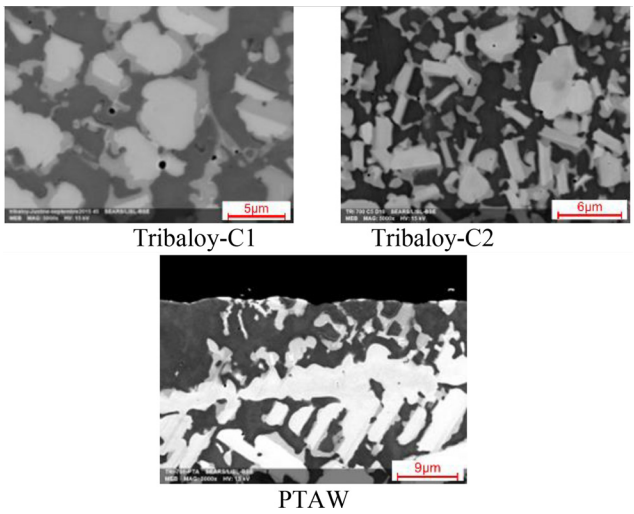

FIG. 9. SEM/BSE images of Tribaloy 700.

subject to discussion because the EDX analysis shows a mix composition of the precipitate that cannot be clearly identified in intermetallic phases as Laves phases.

We observed the same intermetallic phases on the laser sample and the PTAW sample. The main difference between both is the high iron content in the PTAW sample. The iron content decreases from about 25–30 wt. % to the 316L iron content in about 1.5 mm and decreases from about 4–5 wt. % to the surface of the coating.

Deeper investigations by other analysis methods such as transmission electron microscopy or nano-Auger are required for confirming the exact composition of the precipitates.

D. Hardness

The microhardness distribution across the weld clad mapping is shown in Fig. 10. In the PTAW specimen, the microhardness dropped slightly from the substrate (160 $HV_{0.3}$) to the first deposit layer (410 $HV_{0.3}$) overloaded with iron and then we observed a second evolution after about 1500 μm to the second layer (510 $HV_{0.3}$). The sudden variation between the first and second layers is linked to the high dilution of the hard deposited material with the austenitic steel substrate.

In the bounding layer, laser samples have a sudden hardness transition from 160 to 620 $HV_{0.3}$. This abrupt transition is due to the low dilution rate in laser cladding. The level of hardness in the layer deposited by PTAW is lower than laser

TABLE II. SEM/EDS analysis of regions presented in Fig. 8.

Element	Matrix phase (wt. %)	Laves phase (white zone) (wt. %)	Intermediate zone (gray zone) (wt. %)
Ni	60.8	33	39.6
Mo	15.1	50.40	43.7
Cr	19.6	12.00	10.4
Si	1.6	3.80	5.9
Fe	1.9	0.9	0.8
Total	99	100.2	100.4

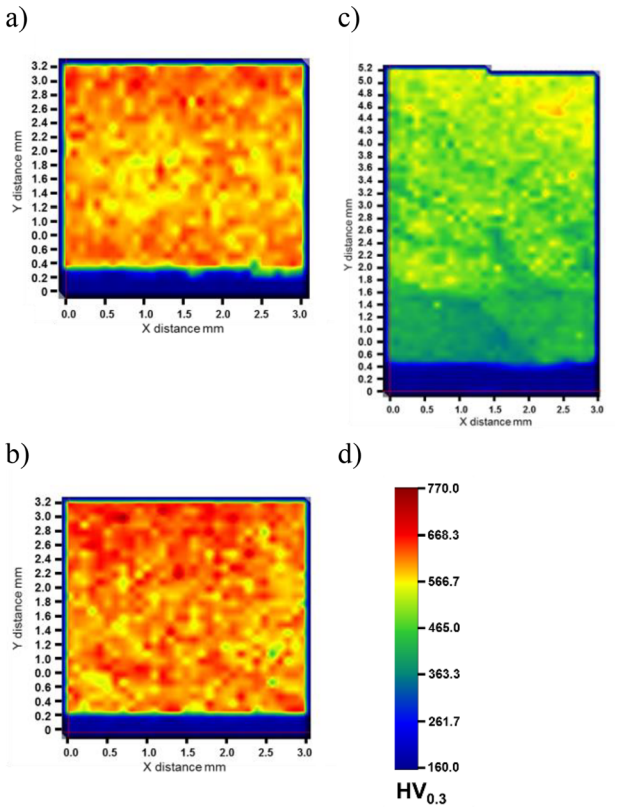

FIG. 10. 2D Vickers microhardness mapping on the vertical cross-section of laser cladding of (a) Tribaloy-C1, (b) Tribaloy-C2, (c) Tribaloy PTAW, and (d) Vickers Hardness color scale ($HV_{0.3}$).

deposited. However, it is more dispersive than the laser. The laser sample hardness is very homogenous.

Differences between the samples have been found in the metallurgical analysis. Then, wear tests have been carried out in order to analyze the wear behavior of the samples.

IV. TRIBOLOGY ANALYSIS FOR TRIBALOY 700

In this section, we present new results on the tribology behavior of Tribaloy 700 alloy made by laser cladding in relation to the process parameters. Tribology tests on other materials can be found in Ref. 12.

The tribological tests were conducted on the TribaloyC2 and Tribaloy-C1 (fixed specimens) deposed on the 316LN steel substrate using a self-made reciprocating tribometer as shown in Fig. 11. A 316LN steel pin with a diameter of 5 mm corresponding to the moving specimens was used as a friction pair. The applied contact stress was 31 MPa. The sliding speed and stroke were 1 mm s^{-1} and 50 mm, respectively, at a temperature of 200 °C and in argon.

The test duration was 10 000 s, resulting in a total sliding distance of 10 m. The tangential forces were recorded during all the test duration and measured using four deformation gauge cells. The mass loss of the worn specimen (moving and fixed) was measured using an analytical balance (an accuracy of 0.1 mg). The surface morphology of specimens was researched using a three-dimensional white light interferometer, a WYKO 3300 NT, and a SEM. The chemical composition of the specimen was analyzed by SEM/EDS.

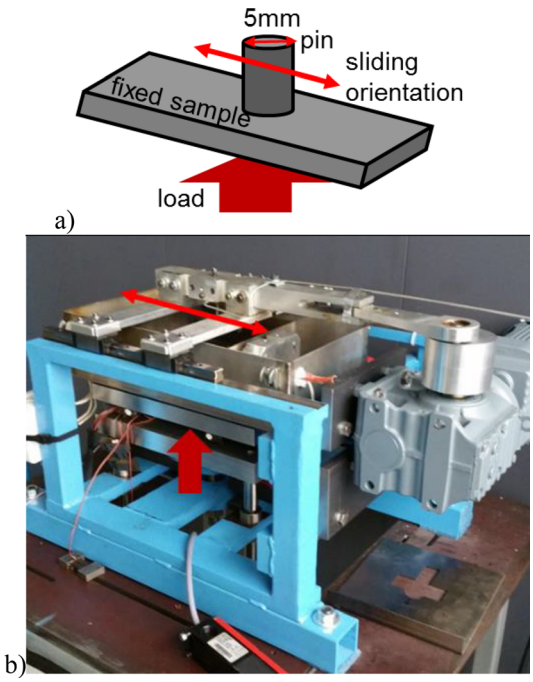

FIG. 11. (a) Geometry of the sliding wear test and (b) photo of the tribometer.

Microhardness was measured at a fixed load of 100 g and a dwell time of 15 s.

The friction coefficient varying with time is presented in Fig. 12. All the friction coefficients have an increase phase in the start stage of sliding, but then each coating has a different trend. Tribaloy-C1 reaches a constant value of 0.65, whereas Tribaloy-C2 decreases from 0.65 to 0.4 during all the test duration. Analysis of worn track (Fig. 12) shows that for the Tribaloy-C2, important quantity of the softer material (in this case, the pin) was found to adhere on the surface

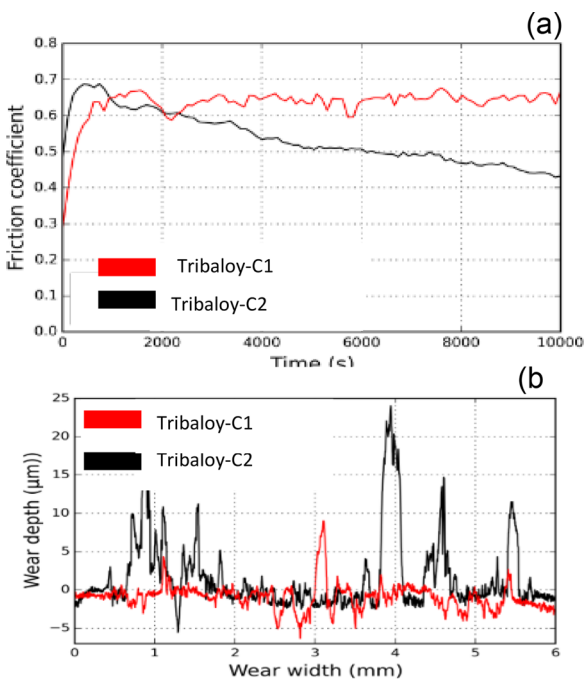

FIG. 12. (a) Friction coefficient and (b) worn track of Tribaloy coating.

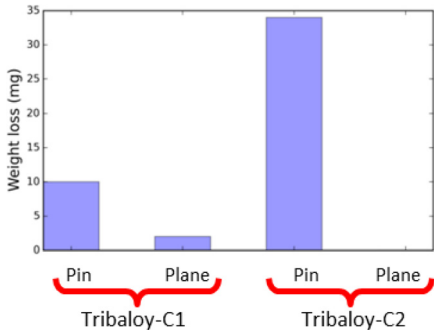

FIG. 13. Weight losses of the pin and Tribaloy samples.

(positive wear depth) unlike the profile of the Tribaloy-C1, which presents some shallow grooves and a very small adhered material.

This adhered material on the Tribaloy-C2 surface could explain the decrease in the friction of the coefficient during the test duration. The weight losses of the pin and Tribaloy confirm this result (Fig. 13). Indeed, the weight losses of the pin used with Tribaloy-C2 are very important (34 mg), whereas for the one used with Tribaloy-C1, they are low (10 mg). For the coating, the weight loss is very low: for Tribaloy-C2, null and for Tribaloy-C1, 2 mg.

Postmortem Vickers microhardness measurements of 100 g have been carried out on the cross-section of the Tribaloy samples after mirror polishing. Microhardness plots for Tribaloy-C1 and Tribaloy-C2 are given in Fig. 14. Tribaloy-C2 shows higher microhardness than Tribaloy-C1. A gradient of hardness is clearly observed close to the sliding surface (from 0 to 300 μm). Tribaloy-C2 reaches a maximum value of 770 $HV_{0.1}$, whereas Tribaloy-C1 reaches 715 $HV_{0.1}$. This hardness gradient means that Tribaloy coating undergoes work-hardening during the friction test.

Worn surface morphologies and SEM/EDS analysis after friction tests for different Tribaloy alloys are presented in Figs. 15 and 16. It is clearly evident that all of them have a common morphology of adhesive wear generating a third body. However, the mechanism of adhesive wear of Tribaloy alloy was not similar. Tribaloy-C1 shows tongue-shape adhesive attachments (positive wear depth in Fig. 12(b)).

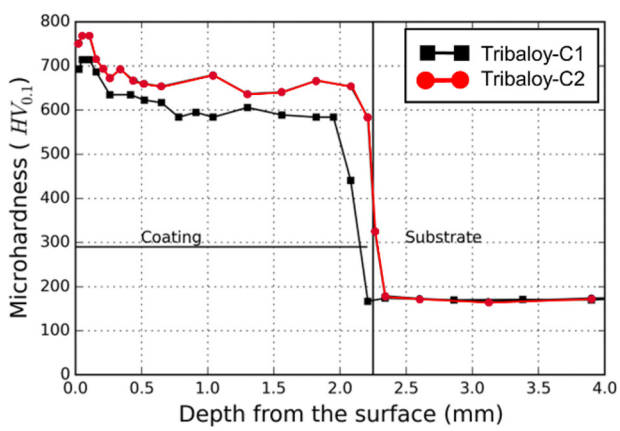

FIG. 14. Microhardness profiles as a function of the distance from the surface.

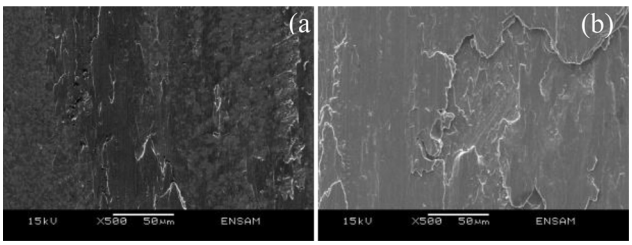

FIG. 15. SEM/SE photograph of the worn surface of (a) Tribaloy-C1 and (b) Tribaloy-C2.

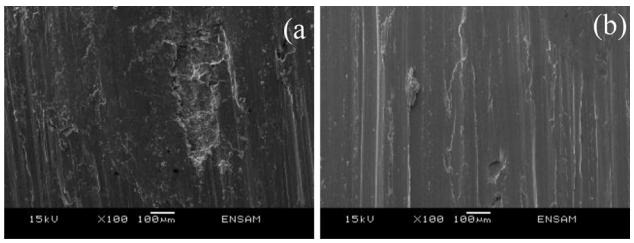

FIG. 17. SEM/SE photograph of the worn surface of the pin used with (a) Tribaloy-C1 and (b) Tribaloy-C2.

The third body was plastically deformed into a tongue shape due to further sliding of mating surfaces: shearing of the third body. The SEM/EDS analysis (Figs. 16(a)–16(c)) reveals a high quantity of iron (white areas of Fig. 16(b)) and a very low quantity of nickel (dark zone of Fig. 16(c)), which indicates a material transfer from the pin. There is also material detachment from the clad layer.

Tribaloy-C2 presents adhesive wear where the third body spreads. The SEM/EDS analysis (Figs. 16(d)–16(f)) reveals a high quantity of iron and a very low quantity of nickel. This third body is principally transferred from the pin. All the surfaces are recovered by the material transferred from the pin. The spreading of this body leads to the growth of the layer until reaching a limited thickness and the debonding of the third body layer.

SEM micrographs of the pin used as a friction pair are presented in Fig. 17. The pin used with Tribaloy-C1 shows a morphology consisting of wear grooves and severe plastically deformed adhesive attachments. SEM/EDS analysis of this pair of friction materials presented in Fig. 18(a) shows that adhesive particles are composed of a mixture of the two materials: Fe, Ni, and Mo are far from the composition of the pin (66% of Fe, 12% of Ni, and 2.3% of Mo). Both the pin and the Tribaloy-C1 have particle detachments resulting in the mixed composition of the third body. This third body could be spread onto both the surfaces acting as lubricants, resulting in a constant value of friction as presented in Fig. 12(a).

The pin used with Tribaloy-C2 shows grooves in the sliding direction corresponding to an abrasive wear. SEM/EDS analysis of the pin wear surface presented in Fig. 18(b) has a similar chemical composition as the material of the pin. There is no transfer from Tribaloy-C2 to the pin but only from the pin to Tribaloy-C2, confirming the high value of the wear loss of the pin and the zero mass loss of Tribaloy-C2 (Fig. 13). Particles transferred from the pin material are spread on the Tribaloy-C2 surface, resulting in a decrease in friction during the test duration (Fig. 12(a)).

It is clear that the variation of the microstructure from C1 to C2 has a significant influence on the wear tests. As it can be seen, the hardnesses of the two samples have a difference of about 50HV. This could partly explain the difference in wear between the two samples. However, the microstructure refinement of the precipitates can also act not only on the hardness but also on other micromechanical effects. This is still under investigation with additional analysis as nanoindentation.

V. CONCLUSION

In this article, we have presented a new study concerning the Cobalt based hardfacing materials for Sodium Reactors. Some nickel based alloys have been selected. The laser cladding process is used for cladding the alloy onto the substrate (316L).

The parameter search has been presented for Tribaloy 700 alloy. We have demonstrated that this alloy can be deposited and that sound clads (no crack, few porosities) can be obtained.

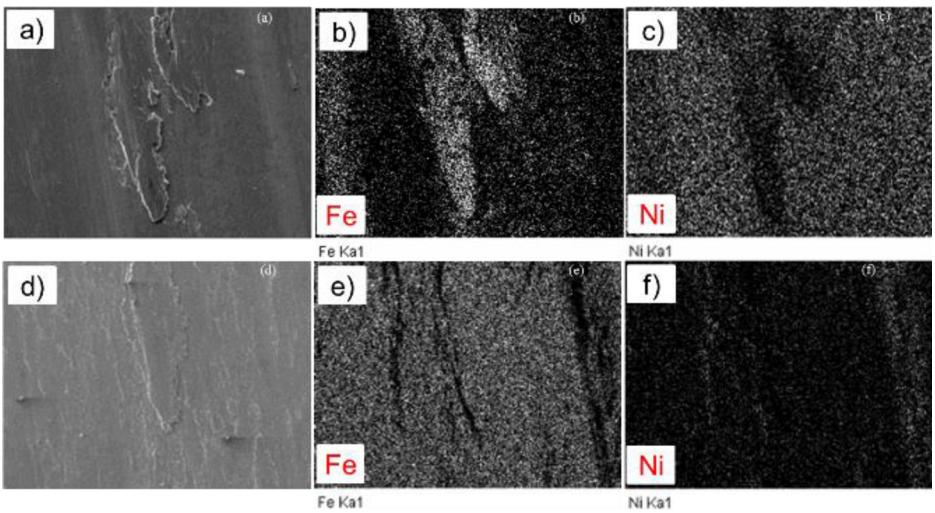

FIG. 16. SEM/EDS analysis of the worn surface of (a)–(c) Tribaloy-C1 and (d)–(f) Tribaloy-C2.

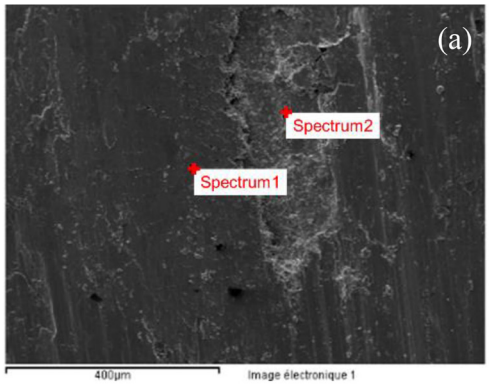

	Weight %			
Spectrum	Cr	Fe	Ni	Mo
1	16.31	39.93	27.31	16.45
2	16.02	20.99	36.62	26.36

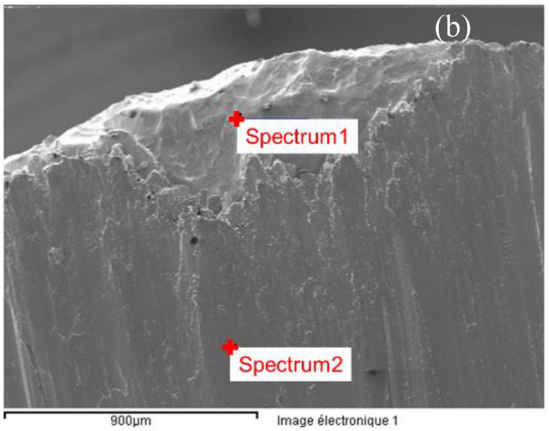

	Weight %			
Spectrum	Cr	Fe	Ni	Mo
1	17.81	70.43	9.05	0.72
2	18.09	65.18	13.08	2.65

FIG. 18. SEM/SE and EDS analysis of the worn surface of the pin used with (a) Tribaloy-C1 and (b) Tribaloy-C2.

The metallurgical analysis exhibits a microstructure globally equiaxed, finer in the case of laser cladding compared to PTAW, with a good homogeneity from the interface to the substrate up to the top of the clad. Hardening phases (Laves phase type) are uniformly dispersed into the material. The nature of the phases, particularly for the Laves phase like structure, has to be more accurately investigated.

The wear tests carried out on two laser cladding samples made with two different travel speeds exhibit quite different wear mechanisms. This demonstrates the capability of the laser cladding process to adapt the quality of the hardfacing material to the tribology conditions and the applications by a variation in the process parameters.

Of course, the corrosion test under sodium and tribo-corrosion tests under sodium at high temperature are required for making a final comparison and validation of the materials. For this, dedicated devices have to be designed and implemented. This will be made later on, after complementary wear tests under argon, etc.

[1]P. M. Dunckley, T. F. J. Quinn, and J. Salter, "Studies of the unlubricated wear of a commercial cobalt-base alloy at temperatures up to about 400 °C," ASLE Trans. **19**, 221–231 (1976).
[2]H. So, C. T. Chen, and Y. A. Chen, "Wear behaviours of laser-clad Stellite alloy 6," Wear **192**, 78–84 (1996).
[3]J. T. M. de Hosson and L. de Mol van Otterloo, *Surface Engineering with Lasers of Co-base Materials, Surface Treatment, Computer Methods and Experimental Measurements* (Computational Mechanics Publications, Southampton, UK, 1997), pp. 341–359.
[4]J. L. de Mol van Otterloo and J. T. M. de Hosson, "Microstructure and abrasive wear of cobalt-based laser coatings," Scr. Mater. **36**, 239–245 (1997).
[5]D. H. E. Persson, S. Jacobson, and S. Hogmark, "Effect of temperature on friction and galling of laser processed Norem 02 and Stellite 21," Wear **255**, 498–503 (2003).
[6]D. H. E. Persson, "Laser processed low friction surfaces," Dissertation for the degree of Licentiate of Philosophy in Materials, Materials Science Division, the Ångström Laboratory, Uppsala University, Sweden, March 2003.
[7]C. B. Bahn, B. C. Han, J. S. Bum, I. S. Hwang, and C. B. Lee, "Wear performance and activity reduction effect of Co free valves, in PWR environment," Nucl. Eng. Des. **231**, 51–65 (2004).
[8]M. Corchia, P. Delogu, and F. Nenci, "Microstructural aspects of wear-resistant Stellite and Colmonoy coatings by laser processing," Wear **119**, 137–152 (1987).
[9]H. Kashani, A. Amadeh, and H. Ghasemi, "Room and high temperature wear behaviors of nickel and cobalt base weld overlay coatings on hot forging dies," Wear **262**, 800–806 (2007).
[10]Q. Ming, L. C. Lim, and Z. D. Chen, "Laser cladding of nickel-based hard-facing alloys," Surf. Coat. Technol. **106**, 174–182 (1998).
[11]D. Kesavan and M. Kamaraj, "The microstructure and high temperature wear performance of a nickel base hardfaced coating," Surf. Coat. Technol. **204**, 4034–4043 (2010).
[12]V. D. Tran, P. Aubry, C. Blanc, J. Varlet, and T. Malot, "Laser cladding and tribocorrosion testing of cobalt-free hardfacing coatings for fast neutron reactor," in *Proceeding of ICALEO 2014* (2014), Paper No. 203.
[13]C. Navas, R. Colaço, J. Damborenea, and R. Vilar, "Abrasive wear behaviour of laser clad and flame sprayed-melted NiCrBSi coatings," Surf. Coat. Technol. **200**, 6854–6862 (2006).
[14]K. Komvopoulos and K. Nagarathnam, "Processing and characterization of laser-cladded coating materials," J. Eng. Mater. Technol. **112**, 131–143 (1990).

Meet the Author

Dr. Pascal J. Aubry is a Senior Expert in Laser Processing at Atomic Energy Commission (CEA). His research activities are mainly related to laser processing, additive manufacturing, surface treatment, and process control.